SHANK2 plays an important role in neuronal polarity

M. M. Versluis[1], R. Kooistra[1], A. Fréal[1,2] & Casper C. Hoogenraad[1,3]

[1] Cell biology, Department of Biology, Faculty of Science, Utrecht University, Padualaan 8, 3584 CH Utrecht, the Netherlands
[2] Department of Axonal Signaling, Netherlands Institute for Neuroscience, Royal Netherlands Academy of Arts and Sciences, Meibergdreef 47, 1105 BA Amsterdam, the Netherlands
[3] Department of Neuroscience, Genentech, Inc., South San Francisco, CA 94080, USA

September 27, 2021

Abstract

SHANK2 is an important scaffolding protein present in the postsynaptic density (PSD) of mature neurons. The PSD region is important for organizing the AMPA and NMDA receptors on the membrane, and for interaction with the cytoskeleton. It is known that SHANK2 plays a role in developmental neuronal diseases, such as autism spectrum disorder. At DIV7 and DIV14 of the development, SHANK2 was found to be present in the axonal growth cones. Here, we characterized the function of SHANK2 in the axonal growth cones. We also questioned whether SHANK2 is present at an earlier stage of the development. This study showed that SHANK2 is present at DIV4 of the development. We found SHANK2 localization in the axonal growth cones, but also in the dendritic growth cones. By performing knockdown experiments, we demonstrate that absence of SHANK2 results in mislocalization of the AIS proteins TRIM46 and AnkG to the dendrites in DIV4 hippocampal neurons. We also observed an altered microtubule organization by overexpressing SHANK2 in COS-7 cells. These results indicate that SHANK2 plays a role in neuronal polarity in early stages of the development, next to its scaffolding role in mature neurons.

Keywords: SHANK2, axon initial segment, TRIM46, Ankyrin G, growth cones, microtubules

Introduction

The hippocampus is a region in the brain, which function is to form connections between neurons to form and retain memories (O'Keefe & Speakman, 1987). Hippocampal neurons present in the hippocampus are key to form these connections and to maintain long-term memory (Guzowski *et al.,* 2000). *In vitro* studies use these hippocampal neurons to gain more insight into the development and function of these hippocampal neurons. Hippocampal neurons start to outgrow neurites from day 1 or 2. After these 1 or 2 days, one neurite will be the longest, this neurite froms the axon. The other neurites become dendrites and start to grow faster after 4 days (Dotti *et al.,* 1998). Growth cones of the neurites are important for this growth, and this growth is established by interactions between the microtubule and actin cytoskeleton (Geraldo & Gordon-Weeks, 2009). The formation of the axons and dendrites begins to define when the neurons become polarized. This means that proteins will be asymmetrically distributed through the neurons (Craig & Banker, 1988).

A region that is important for protein distribution is the axon initial segment (AIS). The main functions of the AIS are to initiate action potential and to maintain neuronal polarity (Coombs *et al.,* 1957; Rasband, 2010). This action potential is essential for communication between neurons. The action potential is initiated by a high density of voltage-gated sodium channels (VGSCs), which localize at the membrane in the AIS (Kole *et al.,* 2008). The protein Ankyrin G (AnkG) binds to

these VGSCs and to microtubules via end-binding (EB) proteins (Fréal *et al.,* 2019; Lemaillet *et al.,* 2003). Therefore, AnkG is one of the key proteins at the AIS, which is important for the formation and maintenance of the AIS (Leterrier *et al.,* 2017). Absence of the scaffolding protein AnkG results in severe restrictions of axon formation (Hedstrom *et al.,* 2008). Another key component of the AIS and important for neuronal polarity is the tripartite motif containing (TRIM) protein, called TRIM46. The function of TRIM46 is to organize the microtubules in parallel to each other by binding to the microtubules. The microtubules are one of the main components of the cytoskeleton and are important for transporting proteins to the axons and dendrites. Absence of TRIM46 results in defects of axon formation and morphology (van Beuningen *et al.,* 2015).

After formation of the AIS and outgrowth of the axon, dendrites start to outgrow during maturation. MAP2 is a member of the microtubule-associated protein (MAP) family, which is found to bind to the microtubules and actin cytoskeleton in the dendrites and soma of the neurons. This binding results in regulation of the stability of the microtubules. The functions of MAP2, and also of another MAP family member Tau, in neurons is to regulate cytoskeletal organization and control morphological changes in neurons. (Dehmelt & Halpain, 2004). Where TRIM46 was found to localize at the AIS between Tau in the axon and MAP2 in the soma and dendrites, AnkG was found as a key player for distribution of MAP2 and Tau (Hedstrom *et al.,* 2008; Sobotzik *et al.,* 2009). Thus, MAP2 and Tau are asymmetrically distributed.

At the end of the maturation, synapses are established in the neurons and therefore neurons can communicate with each other. These communications start with releasing neurotransmitters from the axon terminal of one neuron. These neurotransmitters transport through the synaptic cleft and bind to the α-amino-3-hydroxy-5-methyl-4-isoxazolepropionic acid (AMPA) and N-methyl-D-aspartate (NMDA) receptors of another neuron (Nakanishi, 1992). These receptors are localized on synapses in the dendrites. The AMPA and NMDA receptors are linked to a special region called the postsynaptic density (PSD). In this region, a member of the membrane-associated guanylate kinases (MAGUKs) protein is PSD-95. The function of this protein is to position these receptors correctly on the membrane. PSD-95 is also linked to scaffolding proteins, which indirectly link PSD-95 to the actin cytoskeleton (Chen *et al.,* 2015). The PSD region thus consists of scaffolding proteins, which are linked to the receptors and the actin cytoskeleton.

Another important protein family present in the PSD region is the SHANK family, consisting of three family members SHANK1, SHANK2, and SHANK3. SHANK2 proteins in hippocampal neurons were found to be linked to developmental neuronal diseases, such as autism spectrum disorder (ASD) (Eltokhi *et al.,* 2018; Leblond *et al.,* 2012). Previous studies have found that *de novo* mutations of SHANK2 result in defects in cognitive behavior. These studies showed that SHANK2 mutations resulted in a decrease in spine volume and a decrease in cluster size (Berkel *et al.,* 2010; Berkel *et al.,* 2012). It is therefore important to understand the molecular mechanism and the role of SHANK2 also at early developmental stages.

In young neurons, SHANK2 was found to localize to the axonal growth cones at DIV7 and DIV14 (Halbedl *et al.,* 2016). However, the function of SHANK2 in the axonal growth cones in young neurons is unknown. In mature neurons, SHANK2 functions as scaffolding proteins in the PSD region. The binding with PSD proteins is important to finally position the AMPA and NMDA receptors on the postsynaptic membrane. Other binding domains of SHANK are important to connect the PSD region to the actin cytoskeleton (Naisbitt *et al.,* 1999). The five important binding domains of SHANK are ankyrin repeats (ANK) (McWilliams *et al.,* 2004), scr 3 domain (SH3) (Du *et al.,* 1998), PDZ domain (Boeckers *et al.,* 1999; Naisbitt *et al.,* 1999), proline-rich domain (MacGillavry *et al.,* 2015) and sterile α motif domain (SAM) (Boeckers *et al.,* 2005). The SHANK proteins differ from each other by the order of the repeats, and the use of other promotors and splicing sites (Lim *et al.,* 1999). These domains are important for binding to other proteins in the PSD region. For example,

the interaction of cortactin with the proline-rich domain of SHANK2 regulates the stability of the actin cytoskeleton (MacGillavry *et al.,* 2015). Another important domain of SHANK2 is the PDZ domain, which binds to GKAP and positions the AMPA and NMDA receptors via PSD-95 (Naisbitt *et al.,* 1999).

SHANK2 has 4 different isoforms, called SHANK2A, SHANK2B, SHANK2C, and SHANK2E. These isoforms are formed by alternative splicing and therefore forming different combinations of the binding domains (Lim *et al.,* 1999). In the brain, transcripts indicating the presence of the isoform SHANK2A were found. In epithelial cells, another isoform of SHANK2 was found, which is the longest isoform called SHANK2E (McWilliams *et al.,* 2004). In epithelial cells, the isoform SHANK2E was found to bind to atypical protein kinase C (aPKC), and aPKC forms a complex with PAR3-PAR6. SHANK2E binding to the complex induces formation of the tight junctions and is therefore important for cell polarity (Sasaki *et al.,* 2020). In hippocampal neurons, the aPKC-PAR3-PAR6 complex was found to localize at the axonal growth cones (Shi *et al.,* 2003). PAR3 is transported through the axon to the tip by binding to KIF3A. Additionally, this binding results in binding of aPKC to the PAR3-KIF3A complex (Nishimura *et al.,* 2004). The activity of aPKC at the tip is required for the localization of PAR3, and induces neuronal polarization (Shi *et al.,* 2003). However, it is not known if SHANK2A could bind to this complex in neurons and therefore plays a role in neuronal polarity.

In this study, we examined the function of SHANK2 during the early stages of neurodevelopment. We investigated the distribution of SHANK2, the dynamic behavior of SHANK2, and we investigated what role SHANK2 plays in neuronal polarity. We found endogenous SHANK2 localization at the growth cones of axons and dendrites. We observed that the AIS proteins TRIM46 and AnkG mislocalize to the dendrites when SHANK2 was depleted. However, we found a normal phenotype of the AIS proteins when we rescued the SHANK2 KD with the overexpression constructs of SHANK2 called SHANK2A and SHANK2E. Together, these results imply that SHANK2 plays a role in neuronal polarity.

Results

SHANK2 localizes at the growth cones of young hippocampal neurons

In cultured hippocampal neurons, SHANK2 was found to localize to the axonal growth cones at DIV7 and DIV14, where it colocalizes with the pre-synaptic markers Bassoon and VGluT1 (Halbedl *et al.,* 2016). We examined whether SHANK2 was also present at an earlier stage of neurodevelopment and detected SHANK2 immunostaining already at DIV4. We observed that the SHANK2 signal colocalized with the growth cone marker cortactin in axons (Fig. 1A), indicating that also at this stage, SHANK2 localizes to the axonal growth cones. To verify the specificity of the antibody signal, we induced a SHANK2 knockdown. Therefore, we transfected hippocampal neurons at DIV1 with pSuper-EV as control or with two shRNA's against SHANK2 to induce a SHANK2 knockdown, and immunostained at DIV4. We found that depletion of SHANK2 resulted in a decrease of SHANK2 present in the growth cones of the axon (Fig. 1A). We quantified this by measuring the intensity of SHANK2 in the growth cones and found a significant decrease of SHANK2 signal (fig. 1B), verifying the SHANK2 KD and localization of SHANK2 at the axon growth cones at DIV4.

Interestingly, in the same neurons we also found colocalization of cortactin with endogenous SHANK2 in the dendrites, where the SHANK2 KD neurons demonstrate a decrease of SHANK2 in the growth cones of the dendrites (Fig. 1C). Additionally, we quantified the intensity of SHANK2 in the growth cones and this showed a significant reduction of SHANK2 signal in the SHANK2 KD neurons (Fig. 1D). This indicates that SHANK2 is also present in the growth cones of the dendrites.

We examined whether the decrease in intensity was similar in axons and dendrites by determining the axon/dendrite ratio in all hippocampal neurons. This revealed a significantly lower axon/dendrite ratio of SHANK2 signal in SHANK2 depleted neurons,

indicating a greater decrease of SHANK2 in the axon growth cones (Fig. 1E). This suggests that SHANK2 is present in higher amounts at the axon growth cones. Together, these results suggest that SHANK2 localizes at the growth cones of axons and dendrites in DIV4 hippocampal neurons.

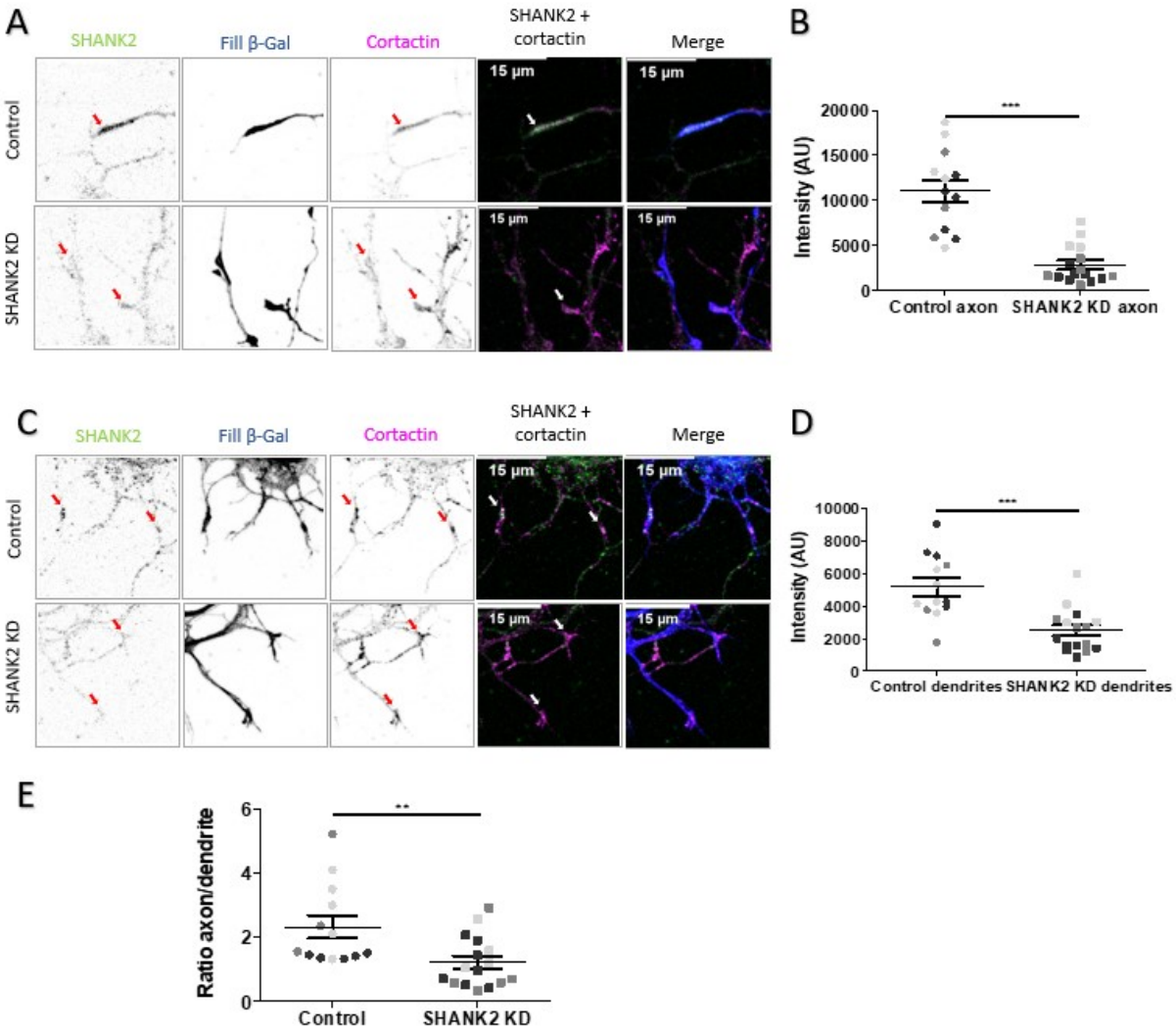

Figure 1. SHANK2 localizes at the growth cones of DIV4 hippocampal neurons.

(A) Representative images of axonal growth cones of DIV4 hippocampal neurons transfected at DIV1 with HA-β-Galactosidase (HA-β-Gal) to visualize the neuron morphology and pSuper-EV as a control (upper panels) or shRNA's against SHANK2 (lower panels), and immunostained for SHANK2 (green), β-Gal (blue) and cortactin (magenta) at DIV4. Arrowheads indicate axon growth cones. Scale bar = 15 µm.

(B) Quantification of SHANK2 levels in the axon of control and SHANK2 KD neurons shown in (A). Different colors indicate data points from independent experiments (N=3, n=13-16); ***p<0.0001.

(C) Representative images of dendrite growth cones of DIV4 hippocampal neurons related to (A). Arrowheads indicate dendritic growth cones. Scale bar = 15 µm.

(D) Quantification of SHANK2 levels in the dendrites of control and SHANK2 KD neurons shown in (C). Different colors indicate data points from independent experiments (N=3, n=13-16); ***p=0.0002.

(E) Axon/dendrite ratio of SHANK2 levels in control and SHANK2 KD neurons. Different colors indicate data points from independent experiments (N=3, n=13-16); **p=0.0078

Data represent mean ± SEM. Unpaired t-test (B, D and E): ns p≥0.05; *p<0.05; **p<0.01; ***p<0.001.

SHANK2 controls localization of the AIS proteins TRIM46 and AnkG

Axonal and dendritic growth cones play a key role in neuronal polarity by elongation of axons and dendrites (Goslin *et al.,* 1988). To examine the function of SHANK2 in growth cones of DIV4 hippocampal neurons, we questioned whether SHANK2 plays a role in neuronal polarity. By inducing a SHANK2 knockdown at DIV1 and perform staining at DIV4 for TRIM46 and AnkG, we determined whether SHANK2 affects the localization of these AIS proteins. In control and SHANK2 KD neurons, TRIM46 and AnkG were found to localize to the AIS. Surprisingly, depletion of SHANK2 also resulted in mislocalization of TRIM46 and AnkG to the dendrites (Fig. 2A). The number of neurons containing mislocalized TRIM46 and AnkG increased from 19 to 65% (Fig. 2B). To check this mislocalization, we quantified the mean intensities of the first 10 µm of three dendrites and the first 26 µm of the axon. While the intensity of TRIM46 and AnkG did not differ in the axon, in the dendrites TRIM46 and AnkG showed a significant increase in intensity (Fig. 2C, 2D). This indicates that SHANK2 could play a role in neuronal polarity.

To further study the effect of SHANK2 on neuronal polarity and the formation of the AIS, we investigated the distribution of the sodium channels. We questioned whether SHANK2 depletion affects localization of the sodium channels. The sodium channels were solely detected in the proximal axon (Fig. 2E, 2F), indicating it is properly targeted to the AIS and does not mislocalize to the dendrites in SHANK2 KD neurons. Although TRIM46 and AnkG mislocalize to the dendrites, the localization of the sodium channels is not affected. We studied the localization of MAP2 to investigate if axons and dendrites are defined. This showed that MAP2 is solely localized in the dendrites and soma (S1). This suggests that SHANK2 induced mislocalization of TRIM46 and AnkG does not affect the formation of the AIS. Subsequently, this indicates that SHANK2 is not important for initiating neuronal polarity but is important for maintaining neuronal polarity.

The induced mislocalization of TRIM46 and AnkG by SHANK2 indicates the importance of SHANK2 in neuronal polarity, and therefore growth of the axon and dendrites. To gain insight into the effect of depletion of SHANK2 on the morphology of hippocampal neurons, we measured the length of all neurites and counted the total number of neurites. We showed that the length of the neurites in SHANK2 depleted neurons was decreased, and the number of neurites increased significantly (Fig. 2G). SHANK2 thus alters the morphology of these hippocampal neurons and therefore could affect the connectivity of hippocampal neurons.

We next studied whether the mislocalization of TRIM46 and AnkG in SHANK2 KD neurons could be rescued by overexpressing the SHANK2 variants SHANK2A and SHANK2E. While in the SHANK2 KD neurons mislocalization was observed for TRIM46 and AnkG, SHANK2 KD neurons rescued with SHANK2A or SHANK2E showed no mislocalization of TRIM46 and AnkG (Fig. 2H). In the SHANK2 KD neurons, we found that 70% of TRIM46 and AnkG were mislocalized. In the rescued neurons containing SHANK2A or SHANK2E, we found mislocalization of TRIM46 and AnkG for 41% and 47% (Fig. 2J). We observed a significant decrease in the number of neurons showing mislocalized TRIM46 and AnkG when SHANK2 KD neurons also overexpressed SHANK2A and SHANK2E. Altogether, these data reveal that SHANK2 plays an important role in maintaining neuronal polarity.

Overexpression of SHANK2 results in AIS localization of TRIM46, AnkG and the sodium channels

To further study the role of SHANK2 in neuronal polarity, we questioned whether overexpression of SHANK2 affects the localization of TRIM46, AnkG, and the sodium channels in DIV4 hippocampal neurons. To validate construct expression, we transfected HEK293 cells with SHANK2A and SHANK2E, and analyzed the expression on the western blot. Western blot analysis showed the presence of SHANK2A and SHANK2E. On the western blot, also other bands are present, which could

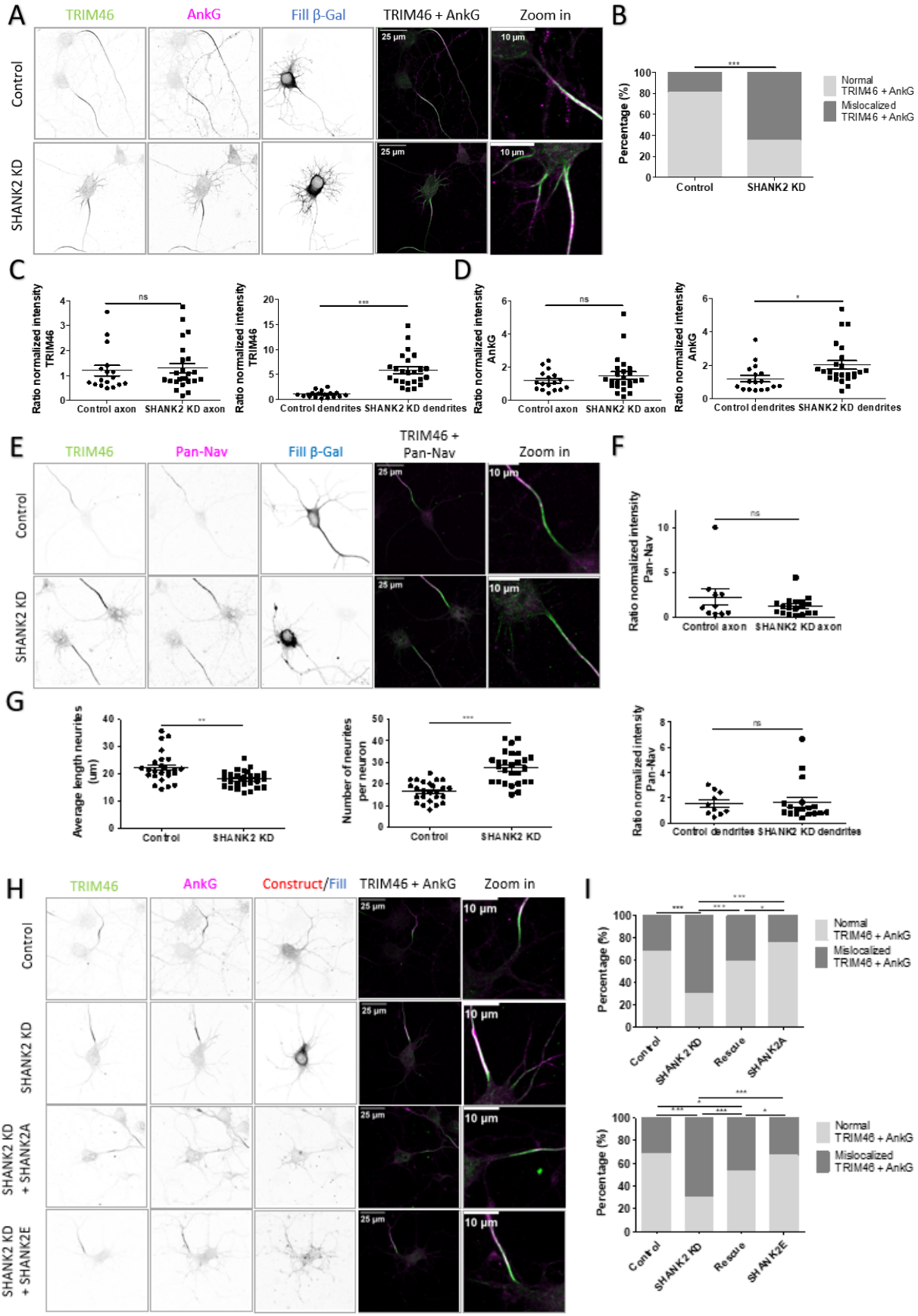

Figure 2. Depletion of SHANK2 results in mislocalization of the AIS proteins TRIM46 and AnkG.

(A) Representative images of DIV4 hippocampal neurons transfected at DIV1 with HA-β-Gal to visualize the neuron morphology and pSuper-EV as control (upper panels) or shRNA's against SHANK2 (lower panels), and

immunostained for TRIM46 (green), AnkG (magenta) and β-Gal (blue) at DIV4. Scale bar = 25 µm and 10 µm (zoom-in).
(B) TRIM46 and AnkG phenotype of transfected neurons shown in (A) were counted. N=3, n=190-406 neurons; ***p<0.0001.
(C) Quantification of TRIM46 levels in the axons and dendrites of transfected neurons related to (A), and normalized to non-transfected neurons. N=3, n=17-24 neurons; ***p<0.0001.
(D) Quantification of AnkG levels in the axons and dendrites of transfected neurons related to (A), and normalized to non-transfected neurons. N=3, n=17-24 neurons; *p=0.0243.
(E) Representative images of DIV4 hippocampal neurons transfected at DIV1 with HA-β-Gal to visualize the neuron morphology and pSuper-EV as control (upper panels) or shRNA's against SHANK2 (lower panels), and immunostained for TRIM46 (green), Pan-Nav (magenta) and β-Gal (blue) at DIV4. Scale bar = 25 µm and 10 µm (zoom-in).
(F) Quantification of the sodium channel levels in the axons and dendrites of the transfected neurons related to (E), and normalized to non-transfected neurons. N=3, n=10-18 neurons.
(G) Quantification of the average length of the neurites and the number of neurites per neuron. Hippocampal neurons were transfected at DIV1 with HA-β-Gal to visualize the neuron morphology and pSuper-EV as control or shRNA's against SHANK2. N=3, n=25-27 neurons; **p=0.0013, ***p<0.0001.
(H) Representative images of DIV4 hippocampal neurons transfected at DIV1 with HA-β-Gal to visualize the neuron morphology, with pSuper-EV as control (first panels), or shRNA's against SHANK2 (second panels), or shRNA's against SHANK2 combined with mCherry-SHANK2A (third panels), or shRNA's against SHANK2 combined with mCherry-SHANK2E (fourth panels). These hippocampal neurons were immunostained at DIV4 for TRIM46 (green), AnkG (magenta) and β-Gal (blue). Scale bar = 25 µm and 10 µm (zoom-in).
(I) TRIM46 and AnkG phenotype of transfected neurons shown in (H) were counted. N=2, n=18-34 neurons. SHANK2A: ***p<0.0001, *p=0.0103. SHANK2E: Control/SHANK2 KD ***p<0.0001, Control/Rescue *p=0.0300, SHANK2 KD/Rescue ***p=0.0010, SHANK2 KD/SHANK2E ***p<0.0001, and Rescue/SHANK2E *p=0.0433.
Chi^2 test and unpaired t-test: ns p≥0.05; *p<0.05; **p<0.01; ***p<0.001. Data represent mean ± SEM.

represent that SHANK2 is degraded. After validation, we induced overexpression of SHANK2 by transfecting DIV1 hippocampal neurons with SHANK2A or SHANK2E constructs, and perform staining for TRIM46 and AnkG at DIV4. SHANK2A and SHANK2E were found to show a punctuate structure, which was also seen for endogenous SHANK2 in young neurons (Fig. 1C, 3B). This could indicate that SHANK2 is transported by vesicles. When investigating the localization of the AIS proteins, we observed no mislocalization of TRIM46 and AnkG in the dendrites (Fig. 3B). SHANK2A and SHANK2E showed no significant difference in the number of neurons containing the normal phenotype of TRIM46 and AnkG. However, the number of neurons containing a normal phenotype of SHANK2A and SHANK2E was decreased compared with control neurons. Where control neurons showed for 92% normal phenotype, overexpression of SHANK2A and SHANK2E showed for 77% and 81% a normal phenotype (Fig. 3C). This suggests that SHANK2A and SHANK2E overexpression in hippocampal neurons does not alter the localization of TRIM46 and AnkG for the majority of the hippocampal neurons.

In addition, we questioned whether SHANK2 overexpression affects the localization of the sodium channels. We induced SHANK2A and SHANK2E overexpression and investigated the distribution of the sodium channels. Detection of the sodium channels was solely found in the axon (Fig. 3D). Examining the percentage of SHANK2 overexpression neurons containing the sodium channels solely in the axon showed no significant difference compared with the control neurons (Fig. 3E). This implies that SHANK2A and SHANK2E overexpression in hippocampal neurons does not alter the localization of the AIS proteins.

To investigate if SHANK2A and SHANK2E overexpression affect the morphology of hippocampal neurons, the number of neurites was counted, and the length of these neurites was measured. This revealed no difference between the average length of the neurites of neurons containing SHANK2A or SHANK2E and control neurons. This implies that overexpression of SHANK2 does not affect the length of the neurites. Counting the number of neurites also showed

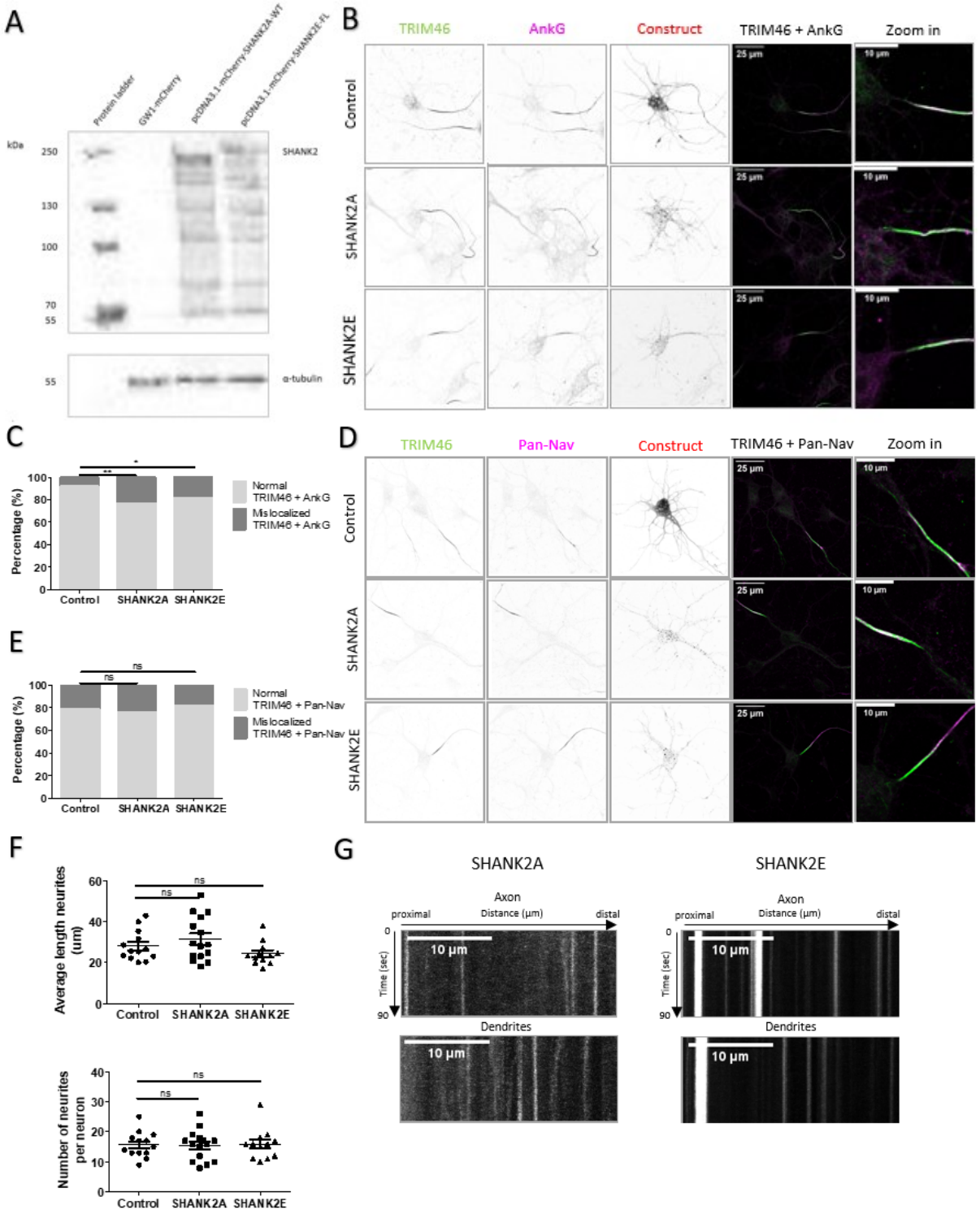

Figure 3. Overexpression of SHANK2A or SHANK2E does not affect the phenotype of AIS proteins.

(A) Western blot analysis of HEK-293 cells transfected with GW1-mCherry as control, mCherry-SHANK2A, mCherry-SHANK2E, and stained for SHANK2 and α-tubulin.

(B) Representative images of DIV4 hippocampal neurons transfected at DIV1 with GW1-mCherry as control (upper panel), mCherry-SHANK2A (middle panel) or mCherry-SHANK2E (lowest panel), and immunostained at DIV4 for TRIM46 (green) and AnkG (magenta). Scale bar = 25 µm and 10 µm (zoom-in).

(C) TRIM46 and AnkG phenotype of transfected neurons shown in (A) were counted. N=2, n=26-40 neurons; *p=0.0228, **p=0.0034.

(D) Representative images of DIV4 hippocampal neurons transfected at DIV1 with GW1-mCherry as control (upper panel), mCherry-SHANK2A (middle panel) or mCherry-SHANK2E (lowest panel), and immunostained at DIV4 for TRIM46 (green) and Pan-Nav (magenta). Scale bar = 25 µm and 10 µm (zoom-in).
(E) TRIM46 and Pan-Nav phenotype of transfected neurons shown in (D) were counted. N=2, n=28-38 neurons.
(F) Quantification of the average length of the neurites and the number of neurites per neuron. Hippocampal neurons were transfected at DIV1 with GW1-mCherry as control, mCherry-SHANK2A or mCherry-SHANK2E. N=3, n=12-15 neurons.
(G) DIV4 hippocampal neurons were transfected at DIV1 with mCherry-SHANK2A or mCherry-SHANK2E. Live imaging was performed at DIV3. The kymographs show the dynamics of SHANK2A and SHANK2E in the axon and in the dendrites in 90 sec. Scale bars = 10 µm.
Chi^2 test: ns $p \geq 0.05$; *$p < 0.05$; **$p < 0.01$; ***$p < 0.001$.

no difference between control and SHANK2A or SHANK2E overexpression neurons (Fig. 3F). This indicates that SHANK2A and SHANK2E overexpression do not alter the morphology of these neurons.

To further examine whether SHANK2 is transported in vesicles, we studied the dynamic behavior of SHANK2A and SHANK2E. We transfected hippocampal neurons with SHANK2A and SHANK2E constructs at DIV1 and investigated the dynamic behavior of SHANK2 by live-cell imaging at DIV3. The kymographs showed that SHANK2A and SHANK2E are mostly static. This is observed in the axons and the dendrites (Fig. 3G). This suggests that SHANK2 is not transported in vesicles.

Altered microtubule organization is observed in COS-7 cells transfected with SHANK2A or SHANK2E

To further determine what role SHANK2 plays in neuronal polarity, we examined the effect of SHANK2 on the microtubules. We used COS-7 cells to observe the effect of SHANK2 on individual microtubules. Therefore, we transfected COS-7 cells with SHANK2A and SHANK2E constructs and studied the stabilization and organization of the microtubules, and colocalization of SHANK2 with the microtubules. We observed SHANK2 localization at the membrane of COS-7 cells, and we did not observe localization of SHANK2 at the microtubules. These observations suggest that SHANK2 does not affect the microtubules directly. In addition, studying the stabilization of microtubules showed that the level of acetylated microtubules was not changed in presence of SHANK2 (Fig. 4A). For the organization of the microtubules, we investigated the effect of SHANK2 on the microtubule organizing center (MTOC). The MTOC is important for maintaining and re-growing of microtubules (Rieder *et al.,* 2001). While in control COS-7 cells we observed the MTOC as a dense structure next to the nucleus, we did not observe this dense structure of MTOC in COS-7 cells containing SHANK2A and SHANK2E (Fig. 4A). Because of the altered microtubule organization, we investigated the effect of SHANK2A and SHANK2E on EB1. EB1 is a plus-end binding (+TIP) protein of the microtubules, which controls microtubule growth (Mimori-Kiyosue *et al.,* 2000). While the microtubule organization was altered, no difference was observed in EB1 density and localization (Fig. 4B). This suggests that SHANK2 is transported to the membrane and that SHANK2 may indirectly alter the microtubule organization.

The role of TRIM46 and SHANK2 on microtubules was investigated, because of the mislocalized TRIM46 in SHANK2 KD neurons and the altered microtubule organization in COS-7 cells containing SHANK2. We transfected COS-7 cells with control GW1-GFP or TRIM46-GFP in combination with GW1-mCherry, mCherry-SHANK2A, or mCherry-SHANK2E. We observed that TRIM46 bundles the microtubules in COS-7 cells. This resulted in absence of the microtubule organizing center, indicating a change in the organization of microtubules. However, adding SHANK2A or SHANK2E to TRIM46 containing COS-7 cells showed no change in the microtubule organization formed by TRIM46 (Fig. 4C). These observations suggest that the microtubule organization is mainly changed by TRIM46.

Because of the direct interaction of cortactin with SHANK2, we investigated the colocalization of cortactin and SHANK2 in COS-7 cells. Overexpression of SHANK2A or

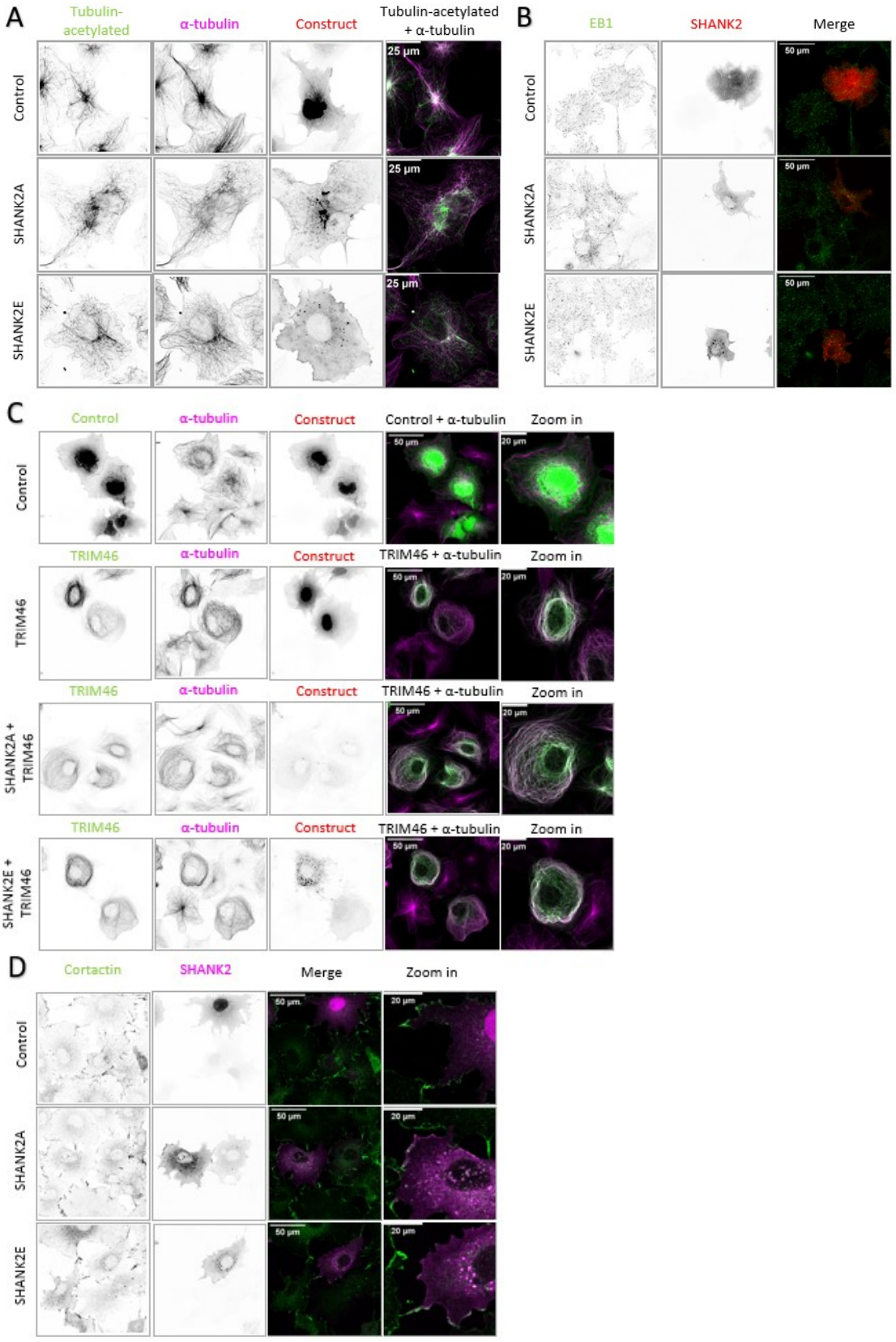

Figure 4. SHANK2 indirectly alters the microtubule organization.

(A) Representative images of COS-7 cells transfected with GW1-mCherry as control, mCherry-SHANK2A, or mCherry-SHANK2E, and immunostained for tubulin-acetylated (green) and α-tubulin (magenta). Scale bar = 25 µm.

(B) Representative images of COS-7 cells transfected with GW1-mCherry, mCherry-SHANK2A, or mCherry-SHANK2E, and immunostained for EB1 (green). Scale bar = 50 µm.
(C) Representative images of COS-7 cells transfected with GW1-mCherry as control, mCherry-SHANK2A or mCherry-SHANK2E, together with GW1-GFP as control or GFP-TRIM46, and immunostained for α-tubulin (magenta). Scale bar = 50 µm and 20 µm (zoom-in).
(D) Representative images of COS-7 cells transfected with GW1-mCherry, mCherry-SHANK2A, or mCherry-SHANK2E, and immunostained for cortactin (green). Scale bar = 50 µm and 20 µm (zoom-in).

SHANK2E resulted in colocalization of cortactin and SHANK2 on the membrane of COS-7-cells (Fig. 4D). This observation suggests that the microtubule organization does not change because of cortactin. These observations together suggest that SHANK2 affects the organization of microtubules indirectly.

No colocalization is observed for SHANK2 and KIF3A

To further study SHANK2 transport, we investigated whether SHANK2 could be transported together with the aPKC-PAR3-PAR6 complex. It is known that aPKC-PAR3 is transported by KIF3A in epithelial cells (Nishimura *et al.,* 2004). Although, we observed static SHANK2, the punctuate structure indicates that SHANK2 could be transported by vesicles (Fig. 1C, 3B, 3G). Therefore, we wanted to investigate whether SHANK2 could be transported by KIF3A by analyzing whether SHANK2 colocalizes with KIF3A. Overexpression of SHANK2A or SHANK2E in COS-7 cells resulted in colocalization of SHANK2 and KIF3A (S2). By transfecting hippocampal neurons at DIV1 with GW1-mCherry as control, SHANK2A, or SHANK2E, and perform staining at DIV4, we investigated this colocalization in hippocampal neurons. We examined whether we could observe colocalization of SHANK2 and KIF3A in the dendrites, dendritic growth cones, the cell body, axonal growth cones, and axons. In the cell body, dendrites, and dendritic growth cones, we did not find colocalization of KIF3A with endogenous SHANK2 in control hippocampal neurons. While we did observe colocalization of SHANK2 with KIF3A in the hippocampal neurons containing SHANK2A and SHANK2E overexpression (Fig. 3A). In addition, we also did not observe endogenous SHANK2 colocalization with KIF3A in the axons and axonal growth cones of control hippocampal neurons. Investigating hippocampal neurons containing SHANK2A or SHANK2E overexpression showed colocalization of SHANK2 with KIF3A (Fig. 5B). These observations suggest that endogenous SHANK2 does not colocalize with KIF3A, and therefore it is likely that SHANK2 is not transported by KIF3A.

Altogether, we showed that SHANK2 localizes to the axonal and dendritic growth cones in DIV4 hippocampal neurons. Depletion of SHANK2 resulted in shorter neurites, which indicates that SHANK2 is important in the axonal and dendritic growth cones for the outgrowth of the neurites. It is known that SHANK2 binds via cortactin to the cytoskeleton, and we showed that overexpression of SHANK2A or SHANK2E in COS-7 cells resulted in an altered microtubule organization. When we studied the AIS and microtubule binding proteins TRIM46 and AnkG in SHANK2 KD neurons, we found mislocalization of TRIM46 and AnkG to the dendrites (Fig. 6). These results together indicate that SHANK2 plays an important role in maintaining neuronal polarity.

Discussion

The role of SHANK2 as a scaffolding protein in the PSD region of mature neurons has been studied extensively (Boeckers *et al.,* 2005; MacGillavry *et al.,* 2016; Naisbitt *et al.,* 1999). A recent study found that SHANK2 was present in the axonal growth cones at DIV7 and DIV14 of the development, indicating that SHANK2 plays a role during the development in the axon (Halbedl *et al.,* 2016). However, the exact role of SHANK2 during the development remained elusive. We found that SHANK2 is present in the axonal and dendritic growth cones of DIV4 hippocampal neurons and that depletion of SHANK2 resulted in defects in neuronal polarity. However, this mislocalization did not appear when SHANK2 KD was rescued with

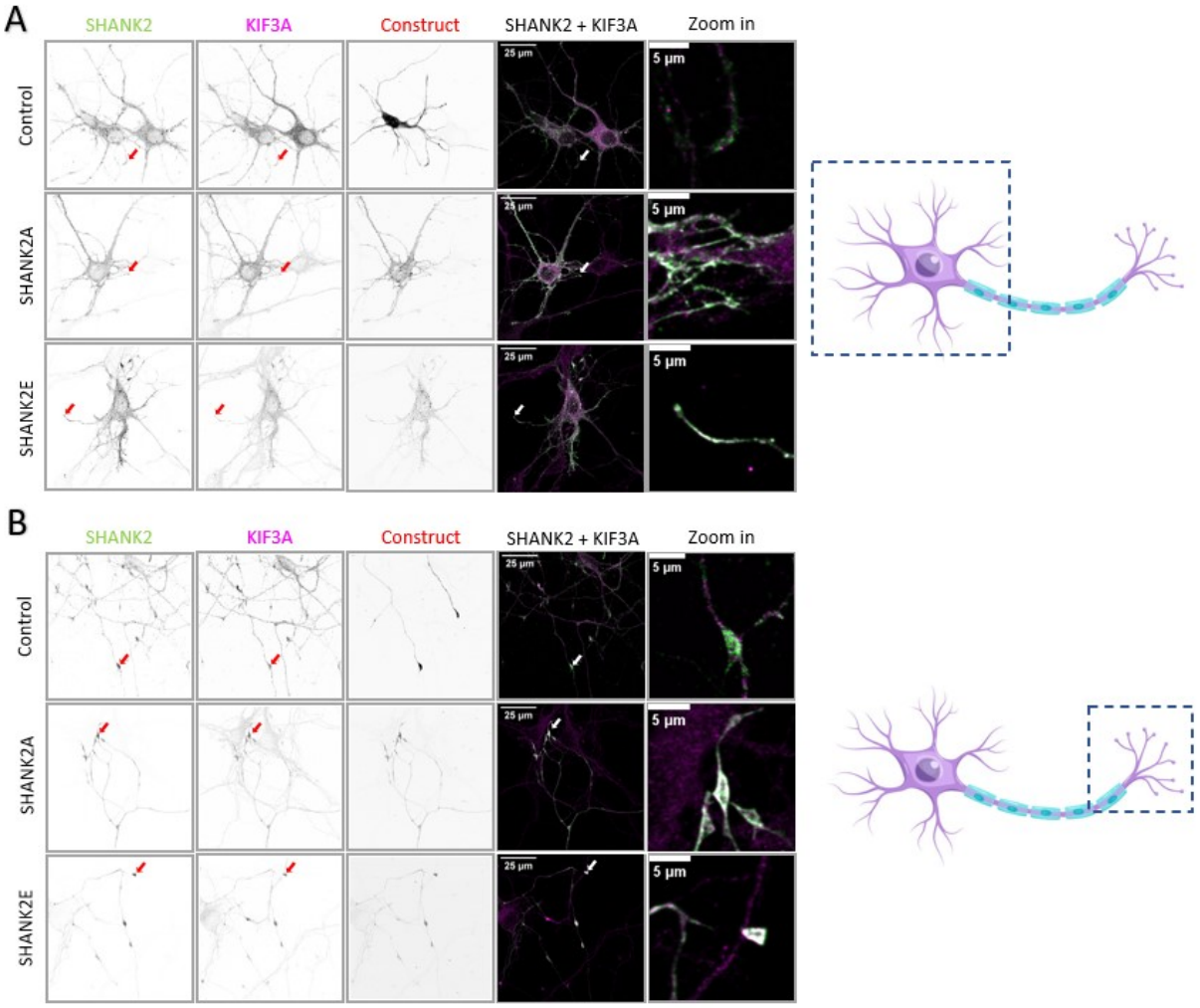

Figure 5. KIF3A does not colocalize with SHANK2 in control neurons.
(A) Representative images of the cell body, dendrites, and dendritic growth cones of DIV4 hippocampal neurons transfected at DIV1 with GW1-mCherry as control, mCherry-SHANK2A, or mCherry-SHANK2E, and immunostained at DIV4 for SHANK2 (green) and KIF3A (magenta). Arrowheads indicate dendritic growth cones. Scale bar = 25 µm and 5 µm (zoom-in).
(B) Representative images of the axonal growth cones of DIV4 hippocampal neurons transfected at DIV1 with GW1-mCherry as control, mCherry-SHANK2A, or mCherry-SHANK2E, and immunostained at DIV4 for SHANK2 (green) and KIF3A (magenta). Arrowheads indicate axonal growth cones. Scale bar = 25 µm and 5 µm (zoom-in).

overexpression of SHANK2A or SHANK2E. This emphasizes the role of SHANK2 in neuronal polarity in early stages of the development, next to its scaffolding role in mature neurons.

The role of SHANK2 in axonal and dendritic growth cones

What exact role SHANK2 plays in neuronal polarity could be speculated when we look at SHANK2 localization at the axonal growth cones. An important complex in neuronal polarity is the aPKC-PAR3-PAR6 complex, which localizes at the axonal growth cones to induce neuronal polarity (Shi *et al.,* 2003). In epithelial cells, when GTPase binds to membrane-localized SHANK2, the complex aPKC-PAR3-PAR6 dissociates. This dissociation results in Rap1 signaling, and subsequently epithelial cell polarity is regulated (Sasaki *et al.,* 2020). We hypothesize that SHANK2 can play a role in neuronal polarity through binding to the aPKC-PAR3-PAR6 complex in axonal growth cones. It would be interesting to investigate whether SHANK2 colocalizes with this complex in the axonal growth cones of young neurons. We

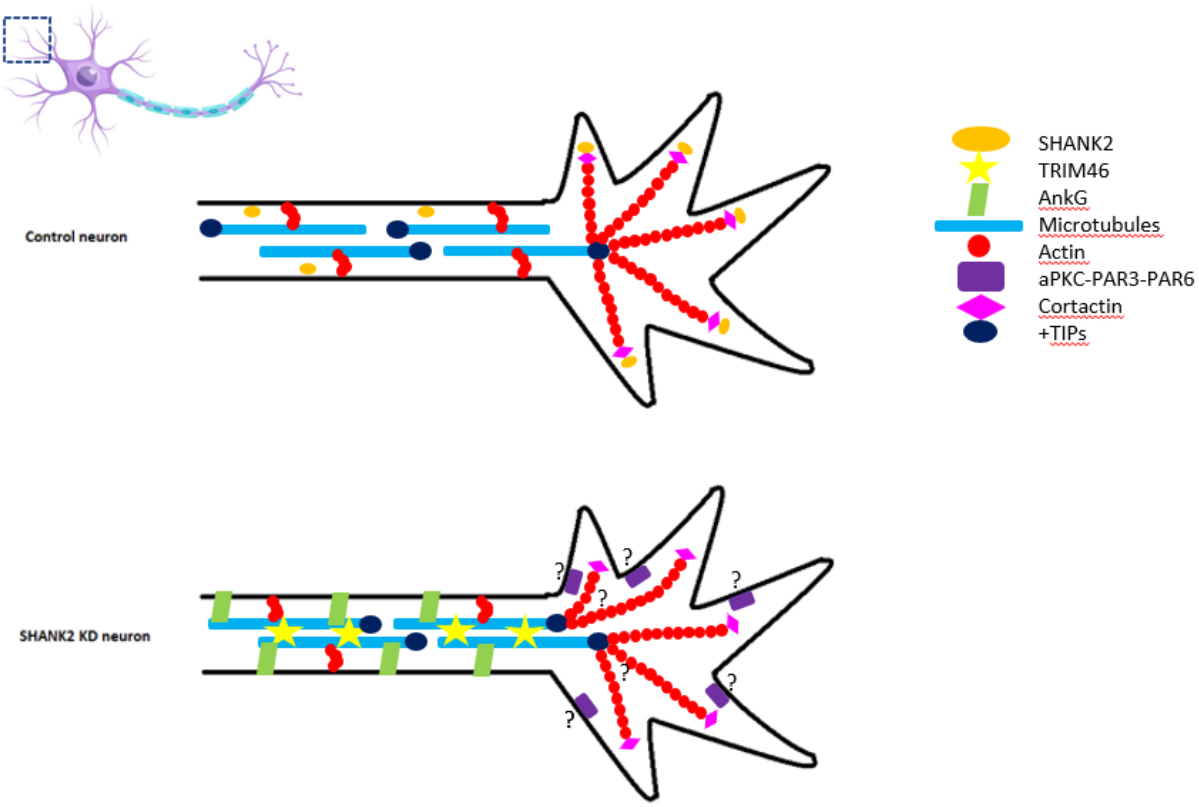

Figure 6. A model of the molecular effects of SHANK2 absence in dendrites.
Schematic overview showing SHANK2 localization at the dendritic growth cones of DIV4 hippocampal neurons. The interactions between the cytoskeleton and SHANK2, cortactin, TRIM46, +TIPS and AnkG in DIV4 control and SHANK2 KD hippocampal neurons are shown.

would expect that absence of SHANK2 results in mislocalization of the complex to the dendrites, because of the role of SHANK2 in neuronal polarity (Fig. 6). We also speculated that SHANK2 could be transported together with aPKC-PAR3 by KIF3A to the axonal growth cones. However, we did not observe colocalization of KIF3A and SHANK2 in hippocampal neurons. This observation suggests that SHANK2 is not transported together with aPKC-PAR3. Whether SHANK2 is transported by KIF3A could be further studied by performing live-cell imaging for colocalization. Another method would be to induce a KIF3A KD to study SHANK2 localization in absence of KIF3A.

We also found SHANK2 in the growth cones of the dendrites in hippocampal neurons at DIV4. SHANK2 is known to localize at the PSD in mature neurons. In addition, SHANK2 was also found to be important for coupling the PSD region to the endocytic zone. Here, SHANK2 regulates metabotropic glutamate receptor 5 and other membrane protein signaling and trafficking (Scheefhals *et al.,* 2019). This showed the importance of SHANK2 in endocytosis in the dendrites. Endocytosis occurs also in the axons, where depletion of TRIM46 was found to affect vesicle transport of AIS proteins and somatodendritic proteins (van Beuningen *et al.,* 2015). This could indicate that absence of SHANK2 results in defects in endocytosis and therefore transport of TRIM46 and AnkG to the dendrites.

In hippocampal neurons, distribution of the endosomatic vesicles is dependent on the microtubules (Parton *et al.,* 1991). In the axon, it is known that the microtubules are uniformly oriented with the plus end towards the growth cones. In contrast, the microtubules in the dendrites are oriented for about 50% towards the growth cones and the

other 50% towards the cell body (Baas *et al.,* 1988). TRIM46 is known to bind to microtubules that are parallel to each other (van Beuningen *et al.,* 2015). This could indicate that the presence of TRIM46 in the dendrites is a result of altered microtubule organization.

The effect of SHANK2 on the AIS proteins

When studying the TRIM46 and AnkG levels in control and SHANK2 KD neurons in the axon, no difference in AIS protein levels was found. In addition, when studying MAP2 distribution in SHANK2 KD neurons, it showed that MAP2 was localized in the soma and dendrites. This implies that the axon and dendrites are defined in the SHANK2 KD neurons. This suggests that neuronal polarity is initiated but could not be maintained in absence of SHANK2. However, there is an increased abundance of TRIM46 and AnkG in the dendrites, which suggests that total levels of these proteins were increased. Further studies could investigate the mRNA levels or whole-cell protein levels in hippocampal neurons by performing a western blot, and for mRNA levels in combination with RNA-sequencing. This could determine the expression levels in control and SHANK2 KD neurons.

Interestingly, we did not find a distribution of the sodium channels to the dendrites in SHANK2 KD neurons. The sodium channels remain localized in the AIS. No observation of the sodium channels in the dendrites could indicate that the number of sodium channels may be too low to detect in the dendrites at this stage. In the AIS, it is known that the sodium channels bind to AnkG (Fréal *et al.,* 2019; Lemaillet *et al.,* 2003). We hypothesize that for this reason, the sodium channels mislocalize together with AnkG and TRIM46. Therefore, it would be interesting to study mRNA levels of the sodium channels by qPCR or to study the localization of the sodium channels in older neurons.

To rescue the phenotype of SHANK2 KD neurons, we used SHANK2A and SHANK2E. We used SHANK2E in hippocampal neurons to investigate whether SHANK2E containing the ankyrin repeats has a different function than SHANK2A, which does not contain the ankyrin repeats. The ankyrin repeats were found to be important in SHANK2E for binding to membrane proteins, and at the membrane, it interacts and regulates the actin cytoskeleton (McWilliams *et al.,* 2004). In neurons, it is known that SHANK2 binds via cortactin to the actin cytoskeleton (MacGillavry *et al.,* 2015). Because of this indirect interaction and the observed altered microtubule organization, it would be interesting to investigate if depletion of SHANK2 results in altered actin organization (Fig. 6).

SHANK2 in health and disease

Because of the known mutations of SHANK2 that play an important role in developmental neuronal diseases, such as autism spectrum disorder (Berkel *et al.,* 2010; Berkel *et al.,* 2012), it is important to give more insight into the roles that SHANK2 plays in health and disease. Our results show that SHANK2 is already present in the growth cones of axons and dendrites of DIV4 hippocampal neurons. Depletion of SHANK2 resulted in defects in neuronal polarity, indicating the importance of SHANK2 in young neurons. Lack of communication between neurons could be explained by shorter neurites forming fewer connections. In addition, defects in asymmetric distribution of proteins could also indicate the lack of communication, because this results in not properly formed axons and dendrites. However, the exact molecular mechanism behind this is still unknown. Therefore, it is important to further study the role of SHANK2 in neuronal polarity and in early development to understand the molecular mechanism behind these diseases, and in health.

Materials and methods

Constructs

In this study, these DNA constructs were used and in detail described previously: GW1-GFP (Hoogenraad *et al.,* 2005), GW1-mCherry (Cunha-Ferreira *et al.,* 2018), pSuper-EV (Brummelkamp *et al.,* 2005), β-actin-HA-βgal (Hoogenraad *et al.,* 2005), pcDNA3.1-mCherry-

SHANK2A-WT (Berkel *et al.,* 2012), and pcDNA3.1-mCherry-SHANK2E-FL (Berkel *et al.,* 2012). Two shRNA's were used to induce a SHANK2 knockdown: shRNA1 with the targeting sequence 5'-GGATAAACCGGAAGAGATA-3' (Berkel *et al.,* 2012) and shRNA2 with the targeting sequence 5'-GGAATTGAGCAAAGAGATT-3' (Berkel *et al.,* 2012). MidiPrep of Quick-start protocol of Qiagen (March 2016) was used for every construct. For this, the QIAGEN Plasmid Midi Kits were used.

Neuron culture

For these experiments, hippocampal neurons from Wister rat embryos were used, which were delivered by Janvier. E18 stage embryos, female and male, were used to obtain hippocampal neurons (Fréal *et al.,* 2019). These hippocampal neurons were placed on laminin (1.25 µg/mL) and poly-L-lysine (37.5 µg/mL) coated 18mm glass coverslips in neurobasal medium (GIBCO) containing 0.5 mM glutamine, 1% penicillin/streptomycin, and 2% B27 (Buijs *et al.,* 2021). The hippocampal neurons were cultured at 37 degrees in 5% CO_2.

For transfection, hippocampal neurons were transfected at days in vitro 1 (DIV1) with 1,8 µg of the constructs and with 3,3 µg of Lipofectamine 2000 (Invitrogen) mixed in 200 µL neurobasal medium. Incubation medium containing 2,5 µL 0,5 mM glutamine for each well is replaced by the neurobasal medium in the 12-wells plate. The 200 µL of incubated lipofectamine with DNA mix was dropwise added to each sample and incubated for 45 minutes. At DIV4, the neurons are fixated with 4% paraformaldehyde (PFA) and 4% sucrose for 10 minutes.

Cell culture

African Green Monkey SV40-transformed kidney fibroblast (COS-7) cells were cultured in DMEM (Lonza) containing 1% penicillin/streptomycin (Sigma) and 10% fetal calf serum (FCS; Sigma) at 37 °C and 5% CO_2. For transfection, a 12-wells plate was used containing COS-7 cells seeded onto 18 mm glass coverslips. After 24 hours, the COS-7 cells were transfected by mixing 100 µL Ham's F10 medium (Lonza) with FuGENE6 (1 µg/µL; Roche) : DNA (1 µg/µL) (2,5:1). This mixture was incubated for 20 minutes at room temperature (RT) and afterward added to the COS-7 cells. The COS-7 cells were incubated for 24 hours at 37 °C and 5% CO_2 before fixation. The COS-7 cells were fixated with 2% methanol and 8% PFA for 10 minutes.

Human embryonic kidney 293 (HEK) cells were also cultured at 37 °C and 5% CO_2 in DMEM (Lonza) containing 1% penicillin/streptomycin (Sigma) and 10% fetal calf serum (FCS; Sigma) at 37 °C and 5% CO_2. For transfection, HEK cells were seeded onto a 10 cm dish. After 24 hours, HEK cells were transfected by mixing polyethylenimine (PEI MAX, PolySciences, Cat# 24765; 1 µg/µL) : DNA (1 µg/µL) (3:1) in Ham's F10 medium. The mixture was incubated for 20 minutes at RT and afterward added to the HEK cells. These cells were incubated for 24 hours before harvesting the HEK cells.

Immunohistochemistry

The primary antibodies used in this study were: guinea pig anti-SHANK2 (Synaptic Systems, Cat# No. 162 204, RRID: AB_2832226; 1:500), rabbit anti-TRIM46 (From C. Hoogenraad lab, homemade van Beuningen *et al.,* 2015; 1:500), guinea pig anti-TRIM46 antibody (Synaptic Systems, Cat# No. 377005; 1:500), rabbit anti-cortactin antibody (Santa Cruz/Bio Connect, Clone H-191, Cat# sc-11408, RRID: AB_2088281; 1:500), chicken anti-β-Gal (Aveslab, Cat# BGL-1040; 1:2000), rabbit anti-GFP (MBL International/Sanbio, clone 081, Cat# 598, RRID: AB_591816; 1:1000), mouse anti-Ankyrin G (Neuromab, clone N106/36, Cat#75-146, RRID: AB_10673030; 1:200), mouse anti-Pan-Nav (Sigma-Aldrich, Clone K58/35, Cat# S8809, RRID: AB_477552; 1:1500), mouse tubulin-α (Sigma-Aldrich, clone B-5-1-2, Cat#T-5168; 1:1000), mouse anti-EB1 (BD Biosciences/Transduction lab, Clone lot:6078948, Cat# 610535, RRID: AB_397892; 1:100), mouse anti-KIF3A (Abcam, Cat# ab11259, RRID: AB_297878; 1:1000), or mouse anti-tubulin-acetylated (Sigma-Aldrich, clone 6-11B-1, Cat# T7451, RRID: AB_609894; 1:600).

The secondary antibodies used in this study were: goat anti-chicken Alexa405 (Abcam/Bioconnect, Cat# ab175675, RRID:

AB_2810980; 1:500), goat anti-rabbit Alexa488 (Life Technologies, Cat# A11034, RRID: AB_2576217; 1:1000), goat anti-rabbit Alexa647 (Life Technologies, Cat# A21245, RRID: AB_2535813; 1:1000), goat anti-guinea pig Alexa488 (Life Technologies, Cat# A11073; 1:1000), goat anti-guinea pig Alexa568 (Life Technologies, Cat# A11075, 1:1000), goat anti-guinea pig Alexa647 (Life Technologies, Cat# A21450; 1:1000), goat anti-mouse Alexa488 (Life Technologies, Cat# A11029, RRID: AB_138404; 1:1000), goat anti-mouse Alexa568 (Life Technologies, Cat# A11031, RRID: AB_14469; 1:1000), goat anti-mouse Alexa 647 (Life Technologies, Cat# A21236, RRID: AB_141725; 1:1000), anti-phalloidin-Alexa488 (Life Technologies, Cat# 0-7466; 1:50), anti-phalloidin-Alexa647 (Life Technologies, Cat# 22287; 1:100). Fluoromount (Invitrogen) was used for mounting the coverslips on glass slides.

Western blot

For western blot, samples were collected from HEK cells. HEK cells were washed in ice-cold PBS, followed by using 1x DTT to scrape and collect the samples. The samples were heated by 95 °C for 10 minutes, put on ice, and then loaded onto a 6% SDS-PAGE gel. After running the gel, the wet blotting system was used to transfer the running gel to a nitrocellulose membrane (Bio-Rad). When the transfer was completed after 1 hour at RT, the membrane was transferred to a tube containing PBS/3% bovine serum albumin (BSA)/0.02% Tween and blocked for 1 hour at RT. Subsequently, the guinea pig anti-SHANK2 (1:1000) and mouse anti-α-tubulin (1:20.000) were used as primary antibodies to probe the western blots. After incubating the primary antibodies at 4 °C overnight, the membrane was washed three times with PBS containing 0.02%Tween and incubated for 1 hour with the secondary antibodies containing a fluorescent tag: anti-guinea pig (IRDye800DX, 1:15.000) and anti-mouse (IRDye680DX, 1:20.000). The scanner Odyssey (LI-COR Biosciences) was used to detect the fluorescence bands on the western blot, followed by analysis by ImageJ/Fiji.

Microscopy

Images of hippocampal neurons and COS-7 cells were obtained by using the confocal fluorescence microscope LSM700 (Zeiss). The objectives used were 63x/1.40 oil and 40x/1.30 oil. The software used for this microscope was ZEN2011 software.

The spinning disk confocal microscope, Nikon Eclipse Ti-E (Nikon), was used for live-cell imaging of hippocampal neurons. The objective used was Nikon Plan Apo VC 60x/1.40 oil and the software used was MetaMorph 7.8 software. An incubator chamber was used to control the temperature at 37 °C and control the CO_2 at 5%. In neurons containing pcDNA3.1-mCherry-SHANK2A-WT and pcDNA3.1-mCherry-SHANK2E-FL, live imaging was performed within a time of 90 seconds, with frames of 1 per second.

Data analysis

Data analysis was performed for quantification and imaging analysis. Blot images and immunofluorescence images were imported to ImageJ/Fiji for analysis and quantification. ImageJ/Fiji was used to compare the mean intensities and colocalization of different proteins.

Quantification SHANK2

For analysis of SHANK2 localization, we quantified the amount of SHANK2 present in the growth cones of axons and dendrites. We drew a line surrounding the growth cones and measured the intensity of SHANK2 in the growth cones. These intensities were subtracted by the background of the image. This was done for images containing control neurons and images containing SHANK2 KD neurons.

Analysis phenotype

For analysis, we counted the number of neurons containing a normal phenotype of TRIM46, AnkG and the sodium channels or a mislocalization of these proteins. These neurons were transfected with pSuper-EV, pcDNA3.1-mCherry-SHANK2A-WT, pcDNA3.1-mCherry-SHANK2E-FL, SHANK2 KD or were rescued. We wrote down for every transfected

neuron whether TRIM46, AnkG and the sodium channels were present in the AIS and/or in the dendrites.

Quantification AIS proteins

To determine the localization and intensity of TRIM46, AnkG, and the sodium channels, a segmented line was drawn through the region of interest. In each image, three dendrites of one transfected neuron and one non-transfected neuron were selected. The first 10 µm of the segmented lines in the dendrites were measured for their mean intensities, which were subtracted by the background. The ratio is determined by dividing the mean intensity of the dendrites of the transfected neuron by the mean intensity of the dendrites of the non-transfected neuron. In the same way, the mean intensity and ratio of the axon were determined. The difference for quantification of the axon is that the first 26 µm were measured.

Kymographs

For the kymographs, a segmented line with a length of 25 µm was drawn through the axon of the hippocampal neurons. The movements of the SHANK2 puncta were measured for 90 seconds, which is shown in the kymograph of the axon. Segmented lines were also drawn with a length of 25 µm through three dendrites of the neurons. Movement of SHANK2 was observed by analysis of the kymographs.

Statistical analysis

Statistical analysis was done by using Excel (Microsoft) and GraphPad Prism 5 (GraphPad Software). From GraphPad Prism 5, the mean ± SEM were obtained and used in the graphs. The values of n, N, and the corresponding test were listed in the figure description. The p value were calculated by doing an unpaired t test or chi^2 test, where ns=not significant; p*<0.05, p**<0.01; and p***<0.001.

Acknowledgement

I want to thank Casper Hoogenraad, Amélie Fréal, and Robbelien Kooistra for this opportunity and for helping me with the experiments and with the analysis. I want to thank Berkel *et al.,* 2012 for sharing the constructs of SHANK2A and SHANK2E.

References

1. Baas, P. W., Deitch, J. S., Black, M. M., & Banker, G. A. (1988). Polarity orientation of microtubules in hippocampal neurons: uniformity in the axon and nonuniformity in the dendrite. *Proceedings of the National Academy of Sciences*, *85*(21), 8335-8339.
2. Berkel, S., Marshall, C. R., Weiss, B., Howe, J., Roeth, R., Moog, U., Endris, V., Roberts, W., Szatmari, P., Pinto, D., Bonin, M., Riess, A., Engels, H., Sprengel, R., Scherer, S. W. & Rappold, G. A. (2010). Mutations in the SHANK2 synaptic scaffolding gene in autism spectrum disorder and mental retardation. *Nature genetics*, *42*(6), 489-491.
3. Berkel, S., Tang, W., Trevino, M., Vogt, M., Obenhaus, H. A., Gass, P., Scherer, S. W., Sprengel, R., Schratt, G., & Rappold, G. A. (2012). Inherited and de novo SHANK2 variants associated with autism spectrum disorder impair neuronal morphogenesis and physiology. *Human molecular genetics*, *21*(2), 344-357
4. van Beuningen, S. F., Will, L., Harterink, M., Chazeau, A., Van Battum, E. Y., Frias, C. P., Franker, M. A. M., Katrukha, E. A., Stucchi, R., Vocking, K., Antunes, A. T., Slenders, L., Doulkeridou, S., Smitt, P. S., Altelaar, A. F. M., Post, J. A., Akhmanova, A., Pasterkamp, J., Kapitein, L. C., de Graaff, E., & Hoogenraad, C. C. (2015). TRIM46 controls neuronal polarity and axon specification by driving the formation of parallel microtubule arrays. *Neuron*, *88*(6), 1208-1226.
5. Boeckers, T. M., Liedtke, T., Spilker, C., Dresbach, T., Bockmann, J., Kreutz, M. R., & Gundelfinger, E. D. (2005). C-terminal synaptic targeting elements for postsynaptic density proteins ProSAP1/Shank2 and ProSAP2/Shank3. *Journal of neurochemistry*, *92*(3), 519-524.
6. Brummelkamp, T. R., Bernards, R., & Agami, R. (2002). A system for stable expression of short interfering RNAs in mammalian cells. *science*, *296*(5567), 550-553.
7. Buijs, R. R., Hummel, J. J., Burute, M., Pan, X., Cao, Y., Stucchi, R., Altelaar, M., Akhmanova, A., Kapitein, L. C., & Hoogenraad, C. C. (2021). WDR47 protects neuronal microtubule minus ends from katanin-mediated severing. *Cell Reports*, *36*(2), 109371.
8. Chen, X., Levy, J. M., Hou, A., Winters, C., Azzam, R., Sousa, A. A., Leapman, R. D., Nicoll, R. A. & Reese, T. S. (2015). PSD-95 family MAGUKs are essential for anchoring AMPA and NMDA receptor complexes at the postsynaptic

density. *Proceedings of the National Academy of Sciences*, *112*(50), E6983-E6992.
9. Coombs, J. S., Curtis, D. R., & Eccles, J. C. (1957). The generation of impulses in motoneurones. *The Journal of physiology*, *139*(2), 232-249.
10. Craig, A. M., & Banker, G. (1994). Neuronal polarity. *Annual review of neuroscience*, *17*, 267-310.
11. Cunha-Ferreira, I., Chazeau, A., Buijs, R. R., Stucchi, R., Will, L., Pan, X., Adolfs, Y., van der Meer, C., Wolthuis, J. C., Kahn, O. I., Schätzle, P., Altelaar, M., Pasterkamp, J., Kapitein, L. C., & Hoogenraad, C. C. (2018). The HAUS complex is a key regulator of non-centrosomal microtubule organization during neuronal development. *Cell reports*, *24*(4), 791-800.
12. Dehmelt, L., & Halpain, S. (2005). The MAP2/Tau family of microtubule-associated proteins. *Genome biology*, *6*(1), 1-10.
13. Dotti, C. G., Sullivan, C. A., & Banker, G. A. (1988). The establishment of polarity by hippocampal neurons in culture. *Journal of Neuroscience*, *8*(4), 1454-1468.
14. Du, Y., Weed, S. A., Xiong, W. C., Marshall, T. D., & Parsons, J. T. (1998). Identification of a novel cortactin SH3 domain-binding protein and its localization to growth cones of cultured neurons. *Molecular and cellular biology*, *18*(10), 5838-5851.
15. Eltokhi, A., Rappold, G., & Sprengel, R. (2018). Distinct phenotypes of Shank2 mouse models reflect neuropsychiatric spectrum disorders of human patients with SHANK2 variants. *Frontiers in molecular neuroscience*, *11*, 240.
16. Fréal, A., Rai, D., Tas, R. P., Pan, X., Katrukha, E. A., van de Willige, D., Stucchi, R., Aher, A., Yang, C., Altelaar, A. F. M., Vocking, K., Post, J. A., Harterink, M., Kapitein, L. C., Akhmanova, A., & Hoogenraad, C. C. (2019). Feedback-driven assembly of the axon initial segment. *Neuron*, *104*(2), 305-321.
17. Geraldo, S., & Gordon-Weeks, P. R. (2009). Cytoskeletal dynamics in growth-cone steering. *Journal of cell science*, *122*(20), 3595-3604.
18. Goslin, K., Schreyer, D. J., Skene, J. P., & Banker, G. (1988). Development of neuronal polarity: GAP-43 distinguishes axonal from dendritic growth cones. *Nature*, *336*(6200), 672-674.
19. Guzowski, J. F., Lyford, G. L., Stevenson, G. D., Houston, F. P., McGaugh, J. L., Worley, P. F., & Barnes, C. A. (2000). Inhibition of activity-dependent arc protein expression in the rat hippocampus impairs the maintenance of long-term potentiation and the consolidation of long-term memory. *Journal of Neuroscience*, *20*(11), 3993-4001.
20. Halbedl, S., Schoen, M., Feiler, M. S., Boeckers, T. M., & Schmeisser, M. J. (2016). Shank3 is localized in axons and presynaptic specializations of developing hippocampal neurons and involved in the modulation of NMDA receptor levels at axon terminals. *Journal of neurochemistry*, *137*(1), 26-32.
21. Hedstrom, K. L., Ogawa, Y., & Rasband, M. N. (2008). AnkyrinG is required for maintenance of the axon initial segment and neuronal polarity. *The Journal of cell biology*, *183*(4), 635-640.
22. Hoogenraad, C. C., Milstein, A. D., Ethell, I. M., Henkemeyer, M., & Sheng, M. (2005). GRIP1 controls dendrite morphogenesis by regulating EphB receptor trafficking. *Nature neuroscience*, *8*(7), 906-915.
23. Kole, M. H., Ilschner, S. U., Kampa, B. M., Williams, S. R., Ruben, P. C., & Stuart, G. J. (2008). Action potential generation requires a high sodium channel density in the axon initial segment. *Nature neuroscience*, *11*(2), 178-186.
24. Leblond, C. S., Heinrich, J., Delorme, R., Proepper, C., Betancur, C., Huguet, G., *et al.,* & Bourgeron, T. (2012). Genetic and functional analyses of SHANK2 mutations suggest a multiple hit model of autism spectrum disorders. *PLoS genetics*, *8*(2), e1002521.
25. Lemaillet, G., Walker, B., & Lambert, S. (2003). Identification of a conserved ankyrin-binding motif in the family of sodium channel α subunits. *Journal of Biological Chemistry*, *278*(30), 27333-27339.
26. Leterrier, C., Clerc, N., Rueda-Boroni, F., Montersino, A., Dargent, B., & Castets, F. (2017). Ankyrin G membrane partners drive the establishment and maintenance of the axon initial segment. *Frontiers in Cellular Neuroscience*, *11*, 6.
27. Lim, S., Naisbitt, S., Yoon, J., Hwang, J. I., Suh, P. G., Sheng, M., & Kim, E. (1999). Characterization of the Shank family of synaptic proteins: multiple genes, alternative splicing, and differential expression in brain and development. *Journal of Biological Chemistry*, *274*(41), 29510-29518.
28. MacGillavry, H. D., Kerr, J. M., Kassner, J., Frost, N. A., & Blanpied, T. A. (2016). Shank–cortactin interactions control actin dynamics to maintain flexibility of neuronal spines and synapses. *European Journal of Neuroscience*, *43*(2), 179-193.
29. McWilliams, R. R., Gidey, E., Fouassier, L., Weed, S. A., & Doctor, R. B. (2004). Characterization of an ankyrin repeat-containing Shank2 isoform (Shank2E) in liver epithelial cells. *Biochemical Journal*, *380*(1), 181-191.
30. Mimori-Kiyosue, Y., Shiina, N., & Tsukita, S. (2000). The dynamic behavior of the APC-binding protein EB1 on the distal ends of microtubules. *Current biology*, *10*(14), 865-868.
31. Naisbitt, S., Kim, E., Tu, J. C., Xiao, B., Sala, C., Valtschanoff, J., Weinberg, R. J., Worley, P. F., & Sheng, M. (1999). Shank, a novel family of postsynaptic density proteins that binds to the

NMDA receptor/PSD-95/GKAP complex and cortactin. *Neuron*, *23*(3), 569-582.
32. Nakanishi, S. (1992). Molecular diversity of glutamate receptors and implications for brain function. *Science*, *258*(5082), 597-603.
33. Nishimura, T., Kato, K., Yamaguchi, T., Fukata, Y., Ohno, S., & Kaibuchi, K. (2004). Role of the PAR-3–KIF3 complex in the establishment of neuronal polarity. *Nature cell biology*, *6*(4), 328-334.
34. O'Keefe, J., & Speakman, A. 1. (1987). Single unit activity in the rat hippocampus during a spatial memory task. *Experimental brain research*, *68*(1), 1-27.
35. Parton, R. G., Dotti, C. G., Bacallao, R., Kurtz, I., Simons, K., & Prydz, K. (1991). pH-induced microtubule-dependent redistribution of late endosomes in neuronal and epithelial cells. *The Journal of Cell Biology*, *113*(2), 261-274.
36. Rasband, M. N. (2010). The axon initial segment and the maintenance of neuronal polarity. *Nature Reviews Neuroscience*, *11*(8), 552-562.
37. Rieder, C. L., Faruki, S., & Khodjakov, A. (2001). The centrosome in vertebrates: more than a microtubule-organizing center. *Trends in cell biology*, *11*(10), 413-419.
38. Sasaki, K., Kojitani, N., Hirose, H., Yoshihama, Y., Suzuki, H., Shimada, M., Takayanagi, A., Yamashita, A., Nakaya, M., Hirano, H., Takahashi, H., & Ohno, S. (2020). Shank2 Binds to aPKC and Controls Tight Junction Formation with Rap1 Signaling during Establishment of Epithelial Cell Polarity. *Cell reports*, *31*(1), 107407.
39. Scheefhals, N., Catsburg, L. A., Westerveld, M. L., Blanpied, T. A., Hoogenraad, C. C., & MacGillavry, H. D. (2019). Shank proteins couple the endocytic zone to the postsynaptic density to control trafficking and signaling of metabotropic glutamate receptor 5. *Cell reports*, *29*(2), 258-269.
40. Shi, S. H., Jan, L. Y., & Jan, Y. N. (2003). Hippocampal neuronal polarity specified by spatially localized mPar3/mPar6 and PI 3-kinase activity. *Cell*, *112*(1), 63-75.
41. Sobotzik, J. M., Sie, J. M., Politi, C., Del Turco, D., Bennett, V., Deller, T., & Schultz, C. (2009). AnkyrinG is required to maintain axo-dendritic polarity in vivo. *Proceedings of the National Academy of Sciences*, *106*(41), 17564-17569.
42. Quick-start protocol MidiPrep (March 2016), www.qiagen.com

Supplementary

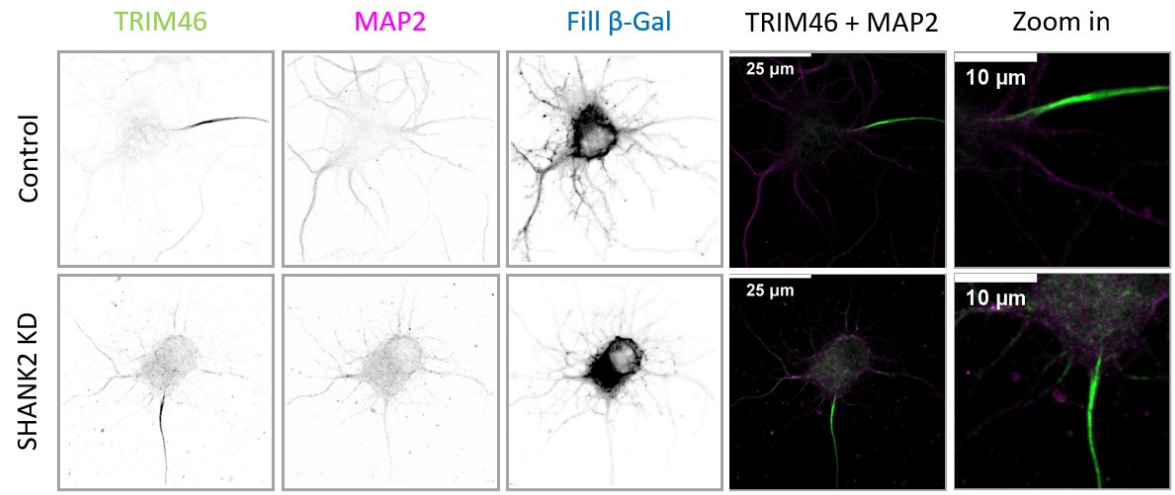

S1. MAP2 is present in the dendrites and soma of control and SHANK2 KD hippocampal neurons.
Representative images of DIV4 hippocampal neurons transfected at DIV1 with HA-β-Gal to visualize the neuron morphology and pSuper-EV as control (upper panels) or shRNA's against SHANK2 (lower panels), and immunostained for TRIM46 (green), MAP2 (magenta) and β-Gal (blue) at DIV4. Scale bars = 25 µm and 10 µm (zoom-in).

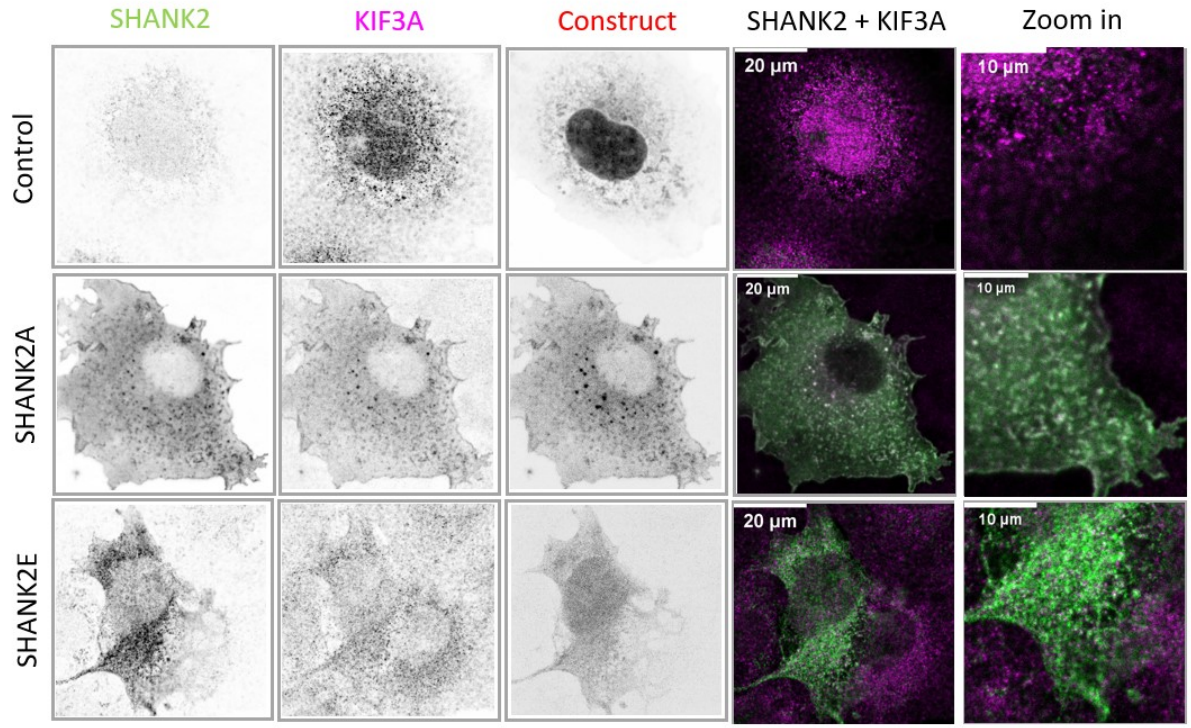

S2. COS-7 cells show colocalization of KIF3A and SHANK2.
Representative images of COS-7 cells transfected with GW1-mCherry as control, mCherry-SHANK2A, or mCherry-SHANK2E, and immunostained for SHANK2 (green) and KIF3A (magenta). Scale bars = 25 µm and 10 µm (zoom-in).

Plain language summary

The hippocampus is a region in the brain, which function is to form and maintain long-term memories. These memories are formed by connections between neurons, called the hippocampal neurons. These hippocampal neurons contain a cell body and many branches called neurites. Neurites contain growth cones, which regulate the growth of the neurites with the help of the cytoskeleton. The cytoskeleton consists of microtubules and actin. Early in the development, one neurite becomes the axon and the other ones become dendrites. The function of the first region of the axon, called the axon initial segment (AIS), is to asymmetrically distribute proteins to the axon, cell body, and dendrites. This asymmetric distribution of proteins is also called neuronal polarity. Important proteins regulating this asymmetric distribution in the AIS are TRIM46, Ankyrin G (AnkG), and the sodium channels.

After maturation, neurons have formed connections with each other. With the help of receptors, which are present on the outer layer of the neuron called the membrane, the neurons can communicate. Molecules from another neuron can bind to these receptors and therefore communication between the neurons starts. These receptors are organized by the region called postsynaptic density (PSD). An important protein present in the PSD is SHANK2. Mutations of SHANK2 were found to be linked to developmental neuronal diseases, such as autism spectrum disorder (ASD). It is therefore important to understand the molecular mechanism and the role of SHANK2 during the development.

We questioned whether SHANK2 is present at early stages of the development. This study showed that SHANK2 is present at DIV4 of the development. At this stage, we showed that SHANK2 is localized at the axonal and dendritic growth cones. Next to this, we also questioned what the role is of SHANK2 in the growth cones. Therefore, we induced a knockdown (KD), which means that in these neurons SHANK2 is depleted. In control neurons, TRIM46 and AnkG were present in the AIS. In neurons containing the SHANK2 KD, we found that TRIM46 and AnkG were present in the AIS, and also in the dendrites. This indicates that absence of SHANK2 results in defects of asymmetric distribution of proteins, and therefore SHANK2 affects neuronal polarity.

We also induced overexpression of SHANK2 in COS-7 cells, which normally do not contain SHANK2. We used COS-7 cells to investigate the individual microtubules, and we observed an altered microtubule organization in SHANK2 presence. This indicates that SHANK2 also affects the microtubule organization. In addition, depletion of SHANK2 in neurons resulted in shorter neurites, which indicates also an effect of SHANK2 on the microtubules. This is because microtubules provide growth, and this observation of shorter neurites implies defects in neurite growth. Altogether, this indicates that SHANK2 plays an important role in neuronal polarity, thus distribution of proteins through the neuron.